

Dynamic Characteristics of Site and Existing Low-Rise RC Building for Seismic Vulnerability Assessment

Kamarudin, A.F., Daud, M.E., Ibrahim, A., Ibrahim, Z. and Koh, H.B.

Abstract— Seismic performance and vulnerability studies of existing reinforced concrete (RC) buildings without seismic design provision in Peninsular Malaysia have been started to be given serious attention. Previous earthquakes from neighboring country of Sumatra and local earthquake events in Bukit Tinggi had shaken many low-rise to high-rise buildings and emerged panic. Insufficient structure durability for excessive lateral resistance, inappropriate building configuration, site-structure resonance effect, poor soil conditions, ground topographic surfaces irregularities etc. may be associated to the building vulnerabilities against seismic threat. In this study, ambient noise measurements were conducted for dynamic characteristics and resonance potential of site and an existing 4-storey RC primary school building of SK Sri Molek in Batu Pahat-Johor (Peninsular Malaysia). Estimations of building capacity and sediment thickness based on the microtremor findings were also discussed. The predominant building frequencies were found between 4.20 Hz and 4.35 Hz in transverse and longitudinal directions, while 2.69 Hz to 3.20 Hz for the ground frequencies, at medium level of resonance potential was estimated. Good agreement and closer prediction of sediment thickness shown in comparison with boreholes data. Since none of specific design response spectra (RS_A) available in the study area, estimation of base shear force using equivalent static analysis (ESA) and Eurocode 8 has been done by substituting the RS_A developed in Kuala Lumpur region. The ultimate horizontal load based on conventional design load combination found to be exceeded 1.5% as provided in BS 8110 which may lead to structural damages.

Keywords— Microtremor, dynamic characteristics, resonance potential, base shear force

This study is supported by Ministry of Education Malaysia (Higher Education) under ERGS grants 011. Special thanks to Universiti Tun Hussein Onn for the equipment and research facilities, JKR, District Education Office of Batu Pahat and SK Sri Molek administration for their priceless cooperation and permission along the period of this research being conducted.

Ahmad Fahmy Kamarudin is a lecturer in Faculty of Civil and Environmental Engineering, Universiti Tun Hussein Onn Malaysia, 86400 Pt. Raja, Bt. Pahat, Johor, MALAYSIA but now pursuing his PhD study in Civil Engineering in similar university (e-mail: afahmy1981@gmail.com).

¹Mohd. Effendi Daud and ²Zainah Ibrahim are the PhD holders and senior lecturers in ¹Faculty of Civil and Environmental Engineering, Universiti Tun Hussein Onn Malaysia, and ²Department of Civil Engineering, Faculty of Engineering, Universiti Malaya, 50603 Kuala Lumpur, MALAYSIA (e-mail: ¹effendi@uthm.edu.my and ²zainah@gmail.com).

Koh Heng Boon is a senior lecturer in Faculty of Civil and Environmental Engineering, Universiti Tun Hussein Onn Malaysia (email: koh@uthm.edu.my).

Azmi Ibrahim is a Phd holder and Professor in Faculty of Civil Engineering, Universiti Teknologi MARA, 40450 Shah Alam, Selangor, MALAYSIA (e-mail: azmii716@yahoo.com).

I. INTRODUCTION

LESS attention has been given to the earthquake hazard especially in low seismic region such as Malaysia. This scenario could be due to previous earthquakes had not inflicted to any severe damage or casualty [4]. Although Peninsular Malaysia is located in the stable Sunda shelf with low to medium seismic activity level, however the effect of tremors from Sumatra earthquakes have been reported several times [5]. According to Megawati, Pan and Koketsu [6], it was predicted that an earthquake at moment magnitude greater than 7.8 from the Sumatra subduction zone has the capability to generate destructive ground motion in Singapore and Kuala Lumpur even at a distance of 700 km. Even a longer distance may create destructive ground motion, it seems reasonable to postulate larger and closer earthquakes that might result in tremendous ground motion to Peninsular Malaysia [7].

Reinforced concrete framed structures had shown in large number of deterioration or become unsafe when subjected to changes in loading and configuration [8]. It is important to take serious action on seismic hazard in order to provide structural and occupant safety especially to the existing RC structure. In the situation of distant earthquake, the seismic waves that reached to Peninsular Malaysia bedrock is rich in long period waves which significantly amplified due to resonance when they propagate upward, especially through the soft soil sites with the frequency close to the predominant frequency of the seismic waves [9]. The amplification waves may cause resonance to the buildings and inducing a large motions on the buildings which enough to be felt by the residence [9]. The site-structure interactions effect due to resonance phenomenon had significantly proven in the destruction of selective buildings between five to fifteen storey which were constructed on the soft ground strata in 1985 Mexico City earthquake [10], even the epicenter distance was approximately 320 km to 350 km away. Therefore, it is important to consider the effect of soil-structure resonance as well either in seismic design or re-evaluation work of existing site or structure even for distant earthquake region due to the tendency of resonance disaster and safety reason.

Microtremor is a non-destructive method, cheap but effective. It is suitable for a region which lack of ground motions records but higher level of noise, for dynamic

characteristics investigation of a ground or structure. The equipment is also light and only small number of operators needed in in-situ measurement [11], at the same time gives extra credit to additional advantages. In this study, microtremor technique was conducted in order to determine the dynamic characteristics of site-structure, level of resonance frequency and seismic vulnerability assessment of existing site and low rise RC building in SK Sri Molek. The dynamic characteristics of site-structure obtained from the microtremor measurements conducted were also validated with some empirical equations, and the base shear force was determined using ESA method. According to Gioncu and Mozzalani [12], ESA is a simplified dynamic analysis and available when there has a predominant mode of vibration (primary mode of vibration) compared to others, and the system is accurately modeled by a single degree of freedom. ESA is an approximation method but adequate for regular building type at the ground fundamental period having close to the first vibration of the structure.

II. STUDY AREA AND FIELDWORK

Fig. 1 shows the location and elevations of SK Sri Molek building. The building is a 4-storey moment resisting RC frame with the masonry wall made by the clay bricks. The school is designed by Public Works Department Malaysia (JKR) based on the standard RC design with typical building configuration of 3.6 m storey height, 3 m spacing between bays, 7.5 m building width and 2.1 m length of cantilever corridor balcony with 1.05 m of parapet wall height. The total length of the building is 60 m.

Each floor is divided into a few rooms as given in Fig. 2. On the upper floor, four main rooms are provided for the prayer room (TBA 6), classroom (TBD 3A), lounge room (TBL 3) and counseling room (TBB 2). Meanwhile, on the second floor, there have a meeting room (TBM 3) and library (TBR10). The headmaster office (TBP 9) and teachers' room (TBT 5) are available on the first floor. Sport room (TSS 3), health centre (TBE 3) and other two classrooms and are placed on the ground floor. The rest rooms with the imposed load used in the calculation of ESA is tabulated in Table 1.

A series of microtremor measurements were performed by using three units of Lennartz portable tri-axial seismometer sensors (S), with 1 Hz eigenfrequency, CityShark II data logger and 1 GB memory flash card. Since the input vibration is based on ambient vibration measured in three major components of NS, EW and vertical (V) directions, the external noise disturbances such as extreme weather (strong wind, lightning, heavy rain etc.), transient noises (traffic, pedestrian, etc.), monochromatic sources (machinery, pumps, generator etc.) and nearby structures (tress, pipes, sewer lids etc.) should be avoided for the best predictions of building and ground natural frequencies as recommended by SESAME [13] guideline. The site-structure measurements were started from 8.00 am and finished at 5.30 pm in five days of fieldwork.

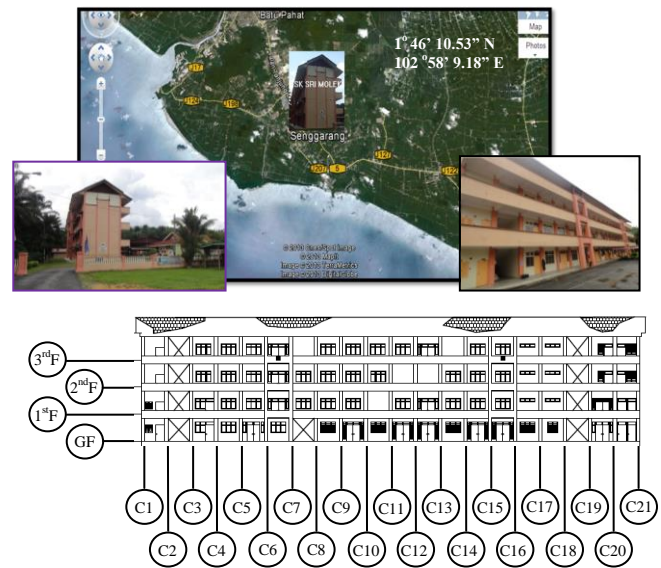


Fig. 1 Specific location and elevations of SK Seri Molek

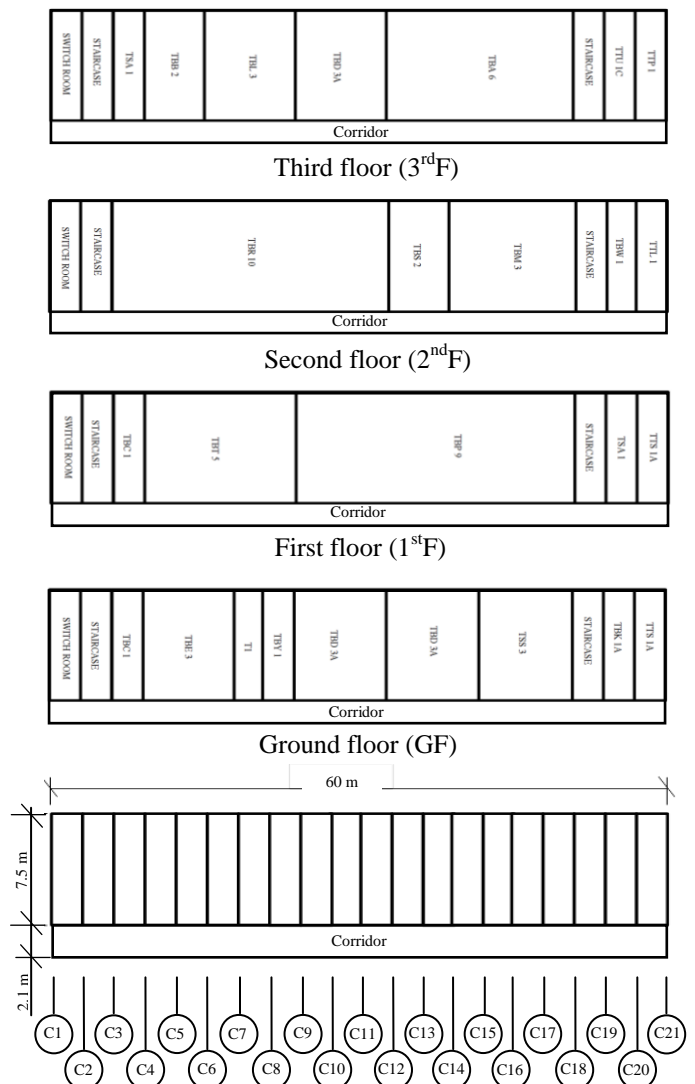


Fig. 2 Floor plans of SK Sri Molek

Similar equipment was applied in both site and building measurements. All sensors were aligned to the True North direction as the bench mark, which parallel to the transverse axis of the building (see Fig. 3). In building measurement, the sensors were arranged in horizontal and vertical sensor alignments closer to the joint of structural members along the corridor. The measurement points of both alignments were tabulated in Table 2 and Table 3. A total of 14 measurements were carried out in horizontal alignment whereas 10 measurements in vertical alignment. Meanwhile, in the site measurement, the sensors were placed on 25 m x 25 m grid as illustrated by six red dots in Fig. 3.

The sampling rate of 100 Hz was used at optimum gain level in all recording. 15 minutes of recording length was taken on site as well as for building. All frequencies below 1 Hz were not of interested [14], for both building and site measurements.

Table 1 Room types in SK Sri Molek building and imposed load, Q_k , used in ESA

Code	Room Function	Q_k (kN/m ²)
TBA 6	Prayer room	3.0
TTU 1C	Wuduk room	2.0
TSS 3	Sport room	2.5
TBL 3	Lounge room	2.5
TBB 2	Counseling room	2.5
TBT 5	Teacher's room	4.0
TBD 3A	Classroom	3.0
TBC 1	Access room	2.0
TBP 9	Headmaster office	4.0
TBM 3	Main meeting room	4.0
TBS 2	Invigilator room	2.5
TBR 10	Library	4.0
TBE 3	Health centre	2.5
TBY 1	Security room	2.0
T 1	Access	2.0
TBK 1A	Book shop	4.0
TBW 1	Prefect Room	2.5
TTP 1	Toilet (Female)	2.0
TTL 1	Toilet (Male)	2.0
TSA 1	Store	2.0
TTS 1 A	Toilet (Staff)	2.0
SWITCH ROOM	Service room	2.0
Corridor	Corridor	3.0

Table 2 Arrangement and position of sensors on every floor in horizontal measurements

Floor No	Sensor 1 (S1)	Sensor 2 (S2)	Sensor 3 (S3)
3rd, 2nd and 1st Floor	C11	C21	C1
	C11	C3	C19
	C11	C6	C16
	C11	C9	C13
Ground Floor	C11	C21	C1
	C11	C16	C6

Table 3 Arrangement and position of sensors at selected columns in vertical measurements

Column No	Sequence of Floor Alignment			
		S1	3 rd	S1
C1, C6, C11, C16, C21	S2	2 nd	S2	2 nd
	S3	1 st	-	-
	-	-	S3	GF

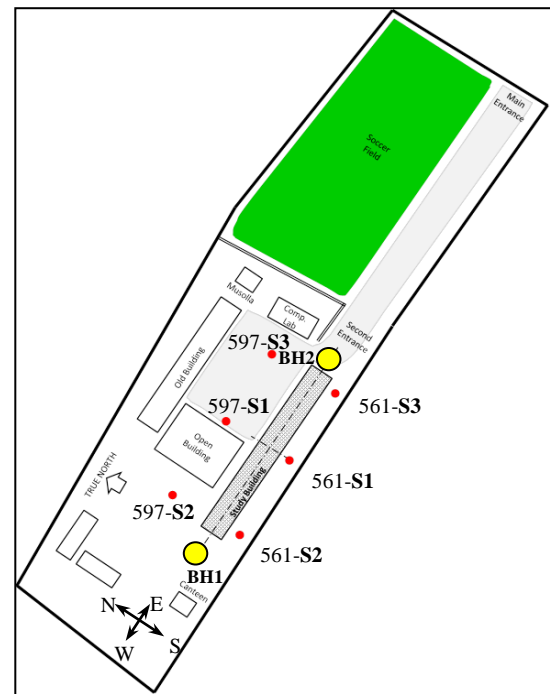


Fig. 3 Layout plan of SK Seri Molek, positions of sensors on ground and borehole (BH) points.

III. DATA PROCESSING AND ANALYSIS

Horizontal to Vertical Spectral Ratio (HVSr) technique is an attractive method especially in estimating the dynamic characteristics of a structure or site in low or none seismicity regions [15]. It is widely used nowadays due to much faster, cheaper and non-destructive compared to conventional methods. Besides, it also proven that the amplification of strong motion at the predominant frequency of ground may approximately estimate through this technique, but in case of larger amplitude of vertical component dominating (when influenced by Rayleigh wave), it may affect to the prediction of amplification characteristic [16]. Besides, HVSr is also not recommended in determination of building frequencies if the soil amplification is significant strong which may contaminate to the building response [17]. Careful analysis and evaluation must be carried out for these reasons. In this study, respective dynamic characteristics estimation for site and building was based on HVSr technique and a standard method of Fourier amplitude spectra (FAS). In order to check the reliability of a building natural frequency, there should has a good correspondence frequency (same frequency on each floor) at each measured floor with the amplitude of peaks predominant frequency will increase with increase of height [17].

Geopsy software was used in the analysis as a processing tool for HVSR and FAS curves analyses based on the following variable parameters; 15 sec of automatic window length was selected with anti-triggering algorithm and a cosine taper of 5%. The Fourier spectra were computed for each window length and smoothed with Konno Ohmachi smoothing constant of 40. Directional energy method was chosen in HVSR analysis when the ambient vibration signals in both NS and EW are calculated accordingly to the respective direction. Reliability and clarity of the significant peaks of mean HVSR curves were checked based on the recommended criteria by the SESAME [13] guideline. The dynamic characteristics in terms of predominant frequency of building, F_o , and fundamental frequencies of ground, f_o , in conjunction with site-structure amplifications, A_o , were picked from the FAS and HVSR curves generated. Illustration of vertical and horizontal building mode shapes were produced based on the predominant frequencies of both longitudinal and transverse directions. From the findings of HVSR curves patterns, f_o and A_o values, further discussions on the sedimentary cover prediction with comparison against two existing borehole profiles were also made.

Estimation of the base shear force was computed using equivalent static analysis according to Eurocode 8 [2]. The intensity of dead load, G_k , and imposed load, Q_k , used were based on typical standard construction design characteristics as proposed by JKR and BS 6399-1 [18]. Since none of a site specific design response spectrum developed in this study region to date, the design response spectrum, RS_A , produced by Looi, Hee, Tsang and Lam in [1] as in Fig. 4 was adopted. The RS_A was modeled based on the consideration of large magnitude distant earthquake of 9.3 from neighboring region of Sumatra with 530 km of the closest to site distance.

The actual notional design ultimate horizontal force that can be resisted by the SK Sri Molek building was calculated to Eurocode 8 [2]. As mentioned in BS 8110 [3], conventional design load combination of $1.4 G_k + 1.6 Q_k$ only allowed to resist a notional design ultimate horizontal load applied at each floor or roof level simultaneously equal to 1.5 % of the characteristic dead weight of the structure between mid-height of the storey below and either mid-height of the storey above or the roof surface.

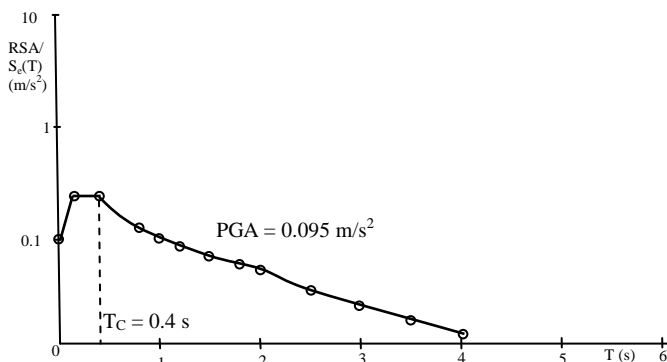


Fig. 4 Redrawn RSA for Kuala Lumpur region [1]

IV. RESULTS AND DISCUSSIONS

A. Dynamic Characteristics of Site and Structure

Table 4 indicates the passing files of site fundamental frequencies (no shaded rows) carried out based on recommendations criteria by SESAME [13] which must fulfilled 3/3 of reliability criteria, and at least 5/6 for clarity criteria from the HVSR curves. The predicted f_o were obtained between 2.69 to 3.20 Hz for the maximum A_o of 7.8 in the NS direction. While, in the EW direction, it shows between 2.79 to 2.98 Hz for the maximum A_o was 7.46. From the evaluation of soil depth for the natural period below < 0.5 s shows that, this site may be classified as shallow stiff soil stratification with 6 to 30 m soil depth based on B&R-M system [19].

The theory and interpretation of ambient vibration for buildings are not so structure and straightforward as for the free-field case (site) [20]. The main difficulty is to detect and eliminate the effects of fundamental frequencies of the nearby free-field and other buildings in the vicinity [20]. Besides, strong site amplification may also able to contaminate the building response and false prediction to the building natural frequencies. Due to these reasons, comparison between FAS (only considered on the upper floor for building) and HVSR (on the ground surface for site) curves in the NS and EW directions were produced for identification of predominant building frequency. Interesting result has shown when the peak FAS curves in the NS direction were slightly shifted to 4.20 Hz (see Fig. 5(a)) but vice versa in the EW direction (see Fig. 6(a)). The site amplifications were highly dominated between 2.69 to 3.20 Hz (see Fig. 5(e)) and 2.79 to 2.98 Hz (see Fig. 6(e)). The first mode of building frequency in the EW was predicted to be occurred at the second peaks frequency of 4.35 Hz which can be clearly seen from the FAS curves. This could be due to high amplifications factor of ground which contaminating to the building response in both directions even though on the highest floor. It was clearly shown from Fig. 5(b)-(d) and Fig. 6(b)-(d), when the peak frequency of FAS curves tend to approach to site's HVSR peak as given in Fig. 5(e) and Fig. 6(e) especially when closing to the bottom level.

Table 4 Reliability and clarity check for of HVSR curves

File No.	Sensor No.	Natural Frequencies, f_o (Hz)	Amplification Factor, A_o	Reliable (R) or No Reliable (NR)	Clear (C) or No Clear (NC)	Criteria: Passed, Failed or Recommended to be Repeated
561-NS	S1	3.20	5.71	R	C	Passed
	S2	2.69	7.78	R	C	Passed
	S3	3.42	9.99	NR	C	Failed
561-EW	S1	2.98	8.32	NR	C	Failed
	S2	2.88	6.78	R	C	Passed
	S3	2.98	7.46	R	C	Passed
597-NS	S1	2.88	7.55	R	C	Passed
	S2	2.79	11.68	NR	C	Failed
	S3	3.20	9.95	NR	C	Failed
597-EW	S1	2.79	6.37	R	C	Passed
	S2	2.79	9.82	NR	C	Failed
	S3	2.88	7.37	R	C	Passed

B. Soil-structure Resonance

Small differences between site and building frequencies possibly trigger to the potential of resonance. The level of soil-structure resonance can be determined by taking the ratio between building frequencies which closer to the site frequency [20]. When the difference is within +15%, the danger of soil-structure resonance is high, if it is within +15 to

25% it is medium, while if it is higher than +25%, then it is low [20].

Table 5 indicates the computed result of site-structure resonance level. From the ratio of 4.20 Hz of building predominant frequency and 3.20 Hz of ground fundamental frequency taken into consideration, it recommends to medium level of resonance potential.

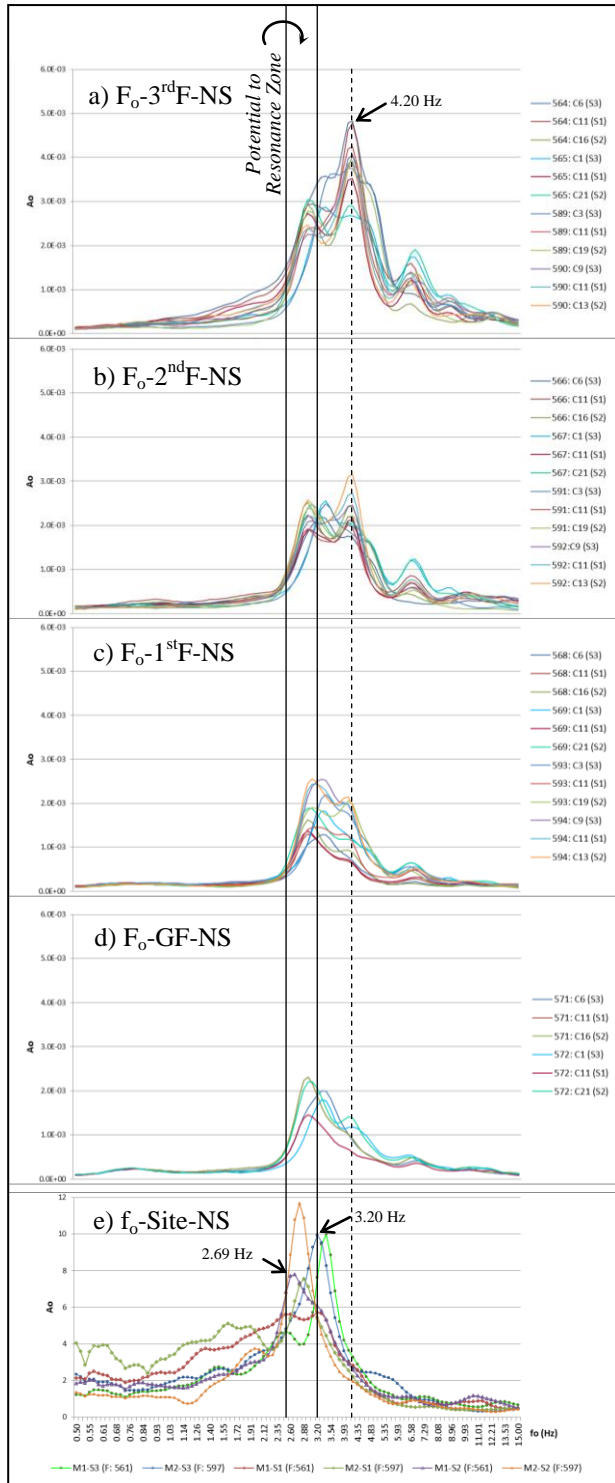


Fig. 5 FAS curves for building and HVSR curves site in the NS direction

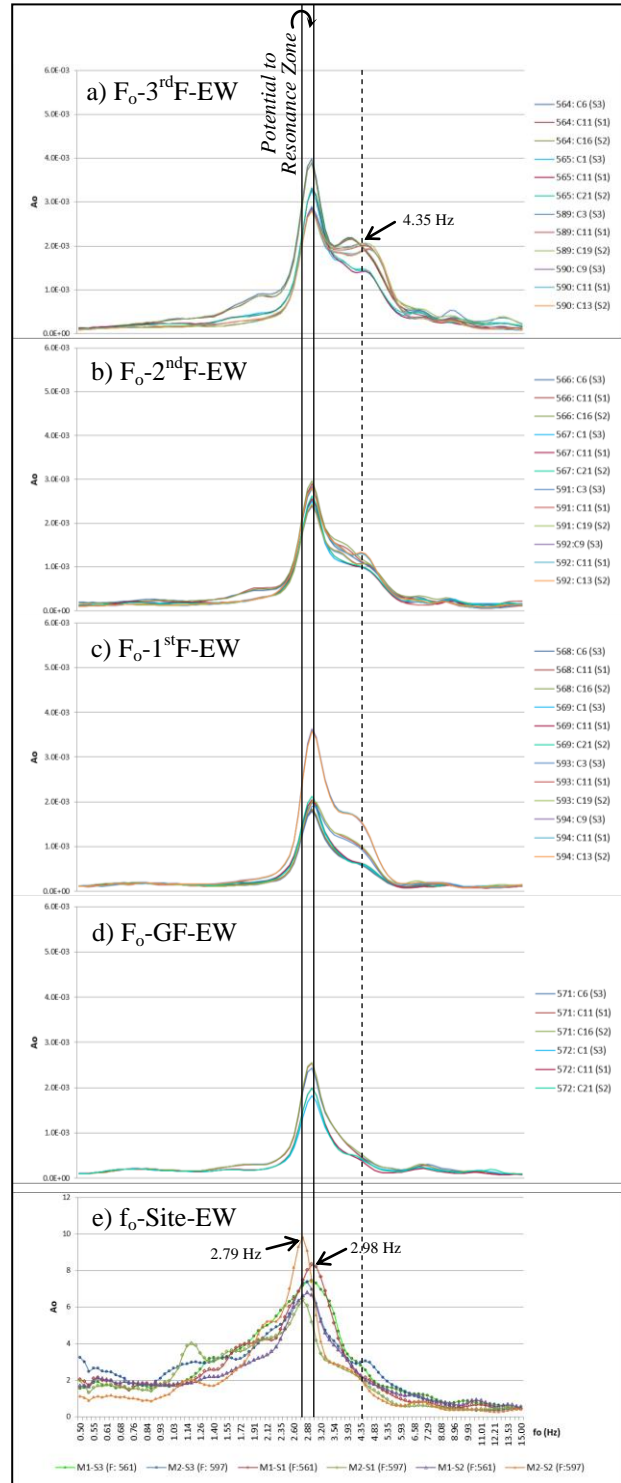


Fig. 6 FAS curves for building and HVSR curves site in the EW direction

Table 5: Site-structure resonance level

	F ₀ (Hz)	f ₀ (Hz)	Danger to Soil-Structure Resonance Potential
NS	4.20	2.6 – 3.20	
EW	4.35	2.98	Medium

C. Mode Shapes

Vertical and horizontal mode shapes were drawn according to the predominant frequencies of building obtained at 4.20 Hz and 4.35 Hz in respective directions. From Fig. 7 and Fig. 8, the displacement pattern of the building showing similar trend when the upper storey remained the highest amplitude and decreasing when lowering to the ground level. Consistent result was also given by the horizontal mode shapes as in Fig. 9 and Fig. 10. Even the school building is geometrically symmetry, but the deformations between bays were slightly different due to several expected reasons as highlighted in following discussions.

By referring to Fig. 7(c) and Fig. 8(c), the center column of C11 has indicated to the highest top displacement in the NS and EW directions, compared to the adjacent column of C6 and C16 on the same floor. This situation is possibly due to higher mass concentration developed at the mid-span in addition to farther distance of the staircases which located in bay two (between C2 to C3) and bay eighteen (between 18 to 19) which less contribute to lateral resistance. Besides, larger imposed loads induced from the classroom (on the 3rd floor) and library (on the 2nd floor) located at the mid-span of the building, may also explained to the sources of the mass. The displacement amplitudes were reducing when reaching to the both ends as illustrated in Fig 7(a)-(b) and 7(d)-(e), as well as Fig. 8(a)-(b) and Fig. 8(d)-(e).

The translational deformation in horizontal mode shapes for both NS and EW directions indicating similar pattern of deformation when the upper floor shows the highest displacement amplitude and getting lesser when lowering to the ground level (see Fig. 9 and Fig. 10).

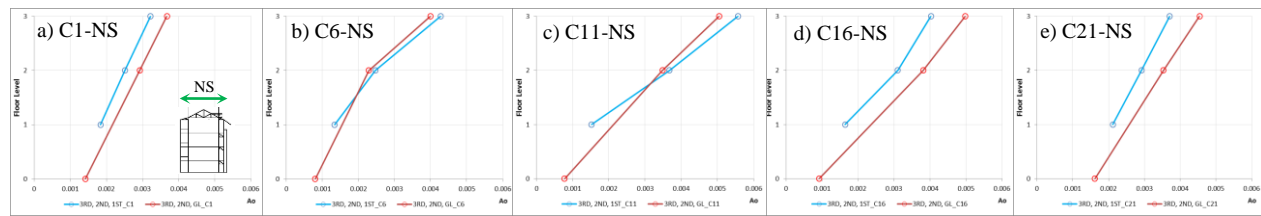


Fig. 7 Dominant vertical mode shape at 4.20 Hz in the NS direction for selective columns

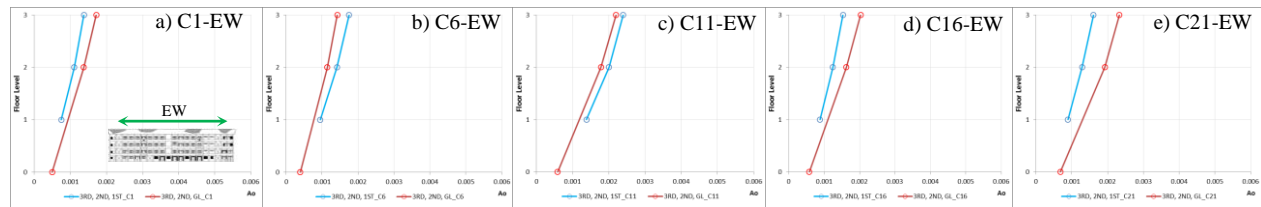


Fig. 8 Dominant vertical mode shape at 4.35 Hz in the EW direction for selective columns

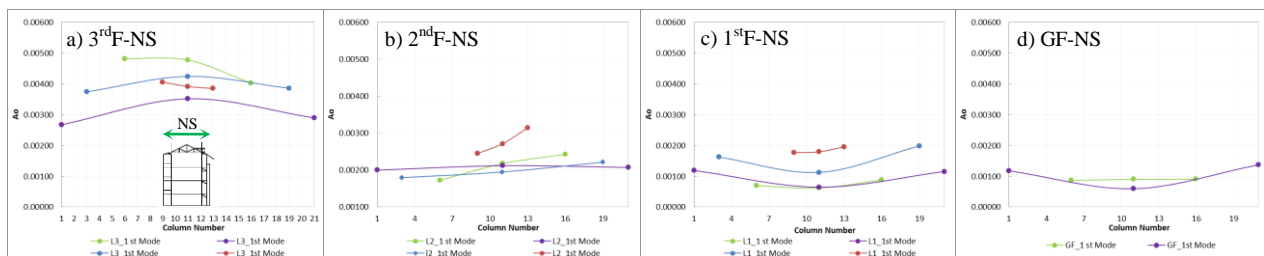


Fig. 9 Horizontal mode shape at 4.20 Hz in the NS direction from the ground floor to upper floor

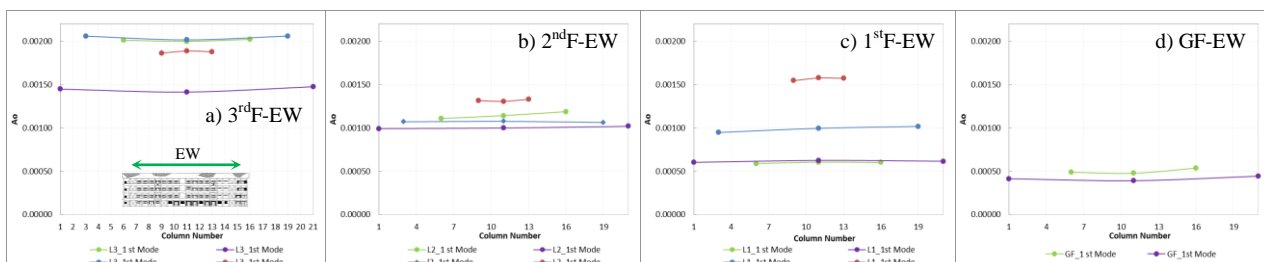


Fig. 10 Horizontal mode shape at 4.35 Hz in the EW direction from the ground floor to upper floor

Inconsistent bending mode shapes were given from the first to the top floors of the building in the NS direction (see Fig. 9(a)-(c)), but steady mode shape was given in the EW direction (see Fig. 10). On the upper floor (see Fig. 9(a)), the maximum displacement amplitude was given at C11 but the amplitudes start reducing when reached to both ends. Vice versa when compared to the deformation in Fig 9(c) at column C11. The amplitudes on the first floor were getting bigger when approaching to the ends. Similar pattern found on the ground level mode shape in Fig. 9(d). This scenario may be affected due to the ground amplification intrusion to the lower levels since higher ground amplification factor were observed at S3 and S2 positions (closer to both wings of the building) compared to the position of S1 (closer to C11).

Finally, in Fig. 10(a)-(d), straight deflection lines were given in all diagrams. However, significant difference was only shown on the first floor (see Fig. 10(c)) when two measurements at C3-C11-C19 and C9-C11-C13 have moved farther than others. The reason was expected due to the external noise disturbance of human activities and car transients on the ground level during the measurement period which may affect the amplitude of the floor displacement.

D. Estimation of Natural Period using Empirical Equations

Estimations of natural period have been made by using three standard codes and previous researches in order to compare the fundamental period of the building obtained from the microtremor measurement. Table 6 shows the prediction equations (Eq.) of natural period (T) where H is the building height above the base in meter for moment resisting frame of RC structure taken from Masi and Vona [21]. The computed results of natural frequency are between 1.85 to 5.00 Hz and the closest prediction has been given by (4).

Table 6 Result comparison between simplified equations and ambient vibration measurement

Code/ Author [21]	Eq.	T (s)	$F_0 = 1/T$ (Hz)	Ambient Vibration Findings, F_0 (Hz)
NEHRP-2003: $T = 0.0466H^{0.9}$	(1)	0.40	2.50 Hz	4.20 Hz to 4.35 Hz at 10.8 m height
ATC3-06 and EC8-CEN2003): $T = 0.075H^{0.75}$	(2)	0.45	2.22 Hz	
NZSEE-2006: $T = 0.09H^{0.75}$	(3)	0.54	1.85 Hz	
Hong and Hwang (2000): $T = 0.0294H^{0.804}$	(4)	0.20	5.00 Hz	

Meanwhile, Table 7 shows a research finding of building frequencies conducted by Gosar [22] for 3 to 5-stories taken from seven buildings. Based on the results, the building frequencies are distributed between 3.1 to 4.8 Hz which consist in the range of this study finding.

Table 7 Natural frequencies of site and building [22]

No.	No. of storey	Year of construction	Building type	Building frequency (Hz)		Soil frequency (Hz)
				Longitudinal	Transverse	
1	5	1962	school	3.4	3.1	3.3
2	3	1908	school	4.2	4.5	4.4
3	3	1911	school	4.4	4.2	4.0
4	5	1965	residential	4.8	3.9	3.9
5	3	1899	school	4.2	3.2	3.9
6	3	1855	school	3.6	3.4	3.5
7	3	1980	health center	3.3	3.3	3.6

E. Estimation of Sediment Thickness based on Ground Fundamental Frequencies

HVSR curves of six measurement points in the NS and EW directions are extracted and arranged as in Fig. 11 (a)-(l). The subsurface soil profile and standard penetration test blow count (SPT 'N') data are traced from the borehole report done by the IKRAM group [23]. HVSR curve of sensors S2 and S3 for measurements file no. 561 and 597 as in Fig. 3 are correlated to the two boreholes as in Fig. 11(m), while the soil profile for S1 is determined from the cross section between BH 1 and BH 2.

The profile of SPT 'N' in Fig. 11(m) were mainly covered from very soft to firm layers up to 18 m approximate depth. Then, the values were significantly increased to medium dense and stiff groups between 15 to 20 m depth. The first 50 blow counts had reached at 21 to 24.2 m depth from the bore logs of BH1 and BH2. Total penetration depths for both boreholes ended at 27 m for BH 1 and 30.5 m for BH 2 with the ground water levels varies from 0.4 to 0.60 m.

Despite from the reliability and clarity criteria of the site fundamental frequencies indicated in Table 4 (the HVSR curves are illustrated as in Fig. 11(a)-(l)) showing failure outcomes and recommended for fieldwork repetition, but all HVSR curves pattern with the present of f_0 and A_0 values may assist for rough picture of geotechnical profile in the NS and EW cross sections. According to Jun [24], a change of the saturation state of the soil layer may have a marked impact on the amplification. The existence of deep soil thickness with a large velocity contrast can be described by a single sharp peak curve as in Figure 11(a) and (c)-(l), whereas shallower soil layers with higher stiffness can be represented by unclear frequency peak from HVSR curve over the whole frequency range as examined in Fig. 11(b).

From the South to the North directions, sharper peak of ground fundamental frequencies are observed based on the pattern of HVSR curves as indicated in Fig. 11 (a), (c), (d) and (f). This may represent to the existence of deeper depth of soil deposit or softer soil layers. Broader HVSR peak curves pattern given by sensor S1, as in Fig 11 (b) and (e) might be explained to the indirect ground improvement due to the pilling groups of the school building, or in other view, the ground may underlain by shallower thickness of sedimentary cover or stiffer layer. Meanwhile, from the East to the West directions, single sharp curve peak pattern are shown in Fig.11 (g)-(l). These HVSR curves pattern can be described by

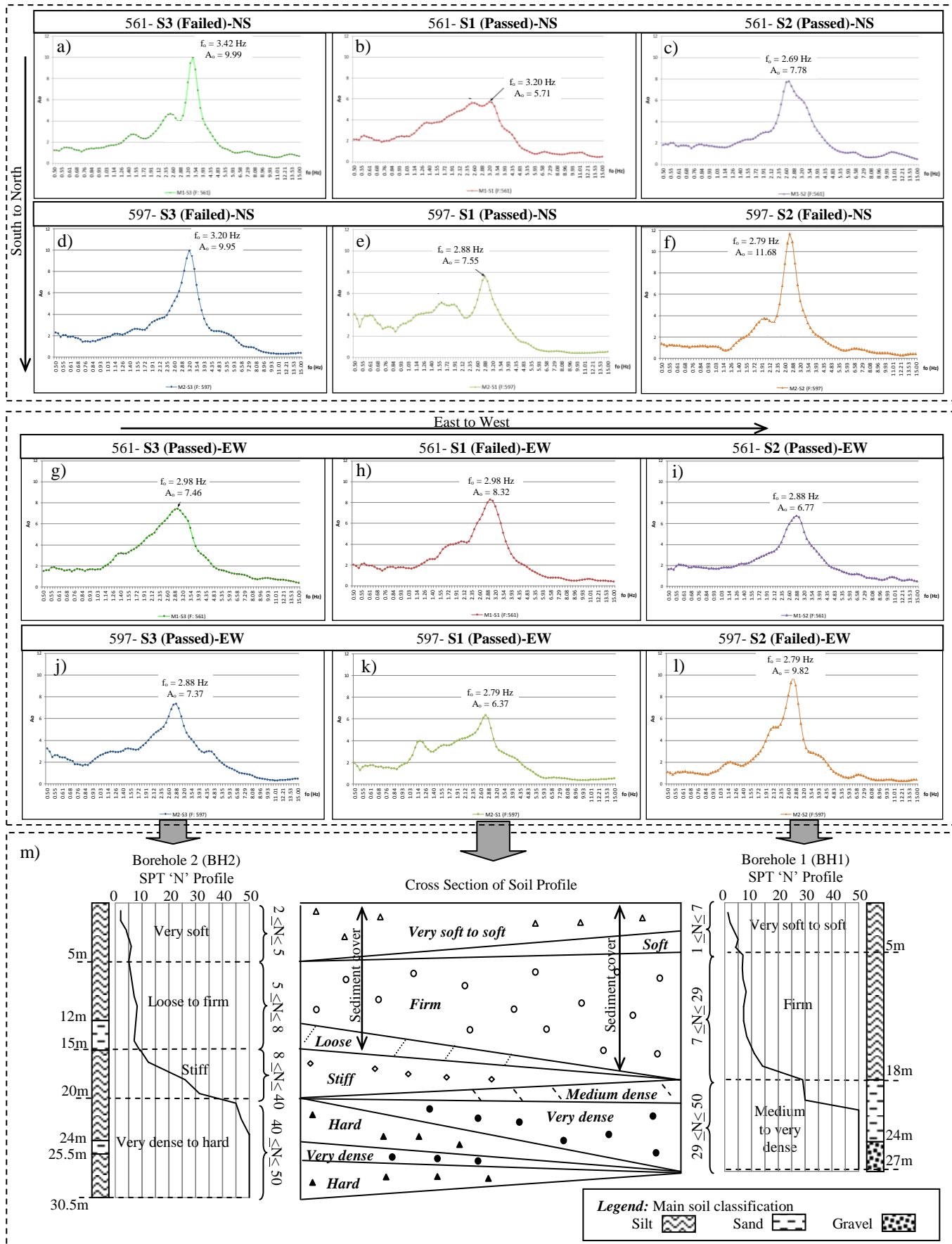


Fig. 11 (a)-(f) HVSR curves in the NS direction, (g)-(l) HVSR curves in the EW direction and (m) SPT 'N' profile and cross section of soil profiles taken from [23]

softer and thicker sedimentary cover with only slight fluctuating between measured points. From the HVSR curve patterns discussed, good agreement indicated when compared to the SPT 'N' profiles given by BH1 and BH2, which consist of 15 to 18 m thickness of very soft to firm soil layers from the ground surfaces.

Microtremor measurement can be used to map the thickness of sediment in several studies, and quantitative relationships between this thickness and the resonance frequency are closely related [25]. As described by the authors in [26], at the location where borehole logs are not available the bedrock profile can be mapped using the observed frequencies of HVSR peaks. In this case, the sediment thickness is defined as soil layer with the shear wave velocity, V_s , smaller than 750 m/s which can be estimated using empirical equation (5), where D is the depth in meters [25]. In order to enhance the validity of the passing site fundamental frequencies obtained against the thickness of sedimentary cover, two empirical equations of (5) and (6) are taken from Motamed, Ghalandarzadeh, Tawhata and Tabatabaei [25] for the shear wave velocity, V_s , and sediment thickness, h , estimations. A comparison between sediment thickness from the microtremors estimation and geotechnical data also provided. Table 8 indicates the computed V_s at multiple depths of BH 1 and BH 2 for shear wave velocity using equation (5). The datum of sediment thickness is determined from the maximum values of V_s can be reached closer to 750 m/s. From the computed results of shear wave velocity, it is clearly shown that the sediment thickness is underlying at 16.7 m depth with SPT 'N' are 13 to 14 from both boreholes.

$$V_s = 134 \text{ SPT}'N^{0.2}D^{0.4} \quad (5)$$

Table 8 Estimation of shear wave velocity for identification of maximum sediment thickness

Borehole	Depth (m)	SPT 'N' blow/cm	Shear wave velocities, V_s (m/s)	Maximum depth of sedimentary cover
BH 1	15.2	11/30	643	
	16.7	14/30	701	/
	18.2	29/30	839	
BH 2	15.2	9/30	618	
	16.7	13/30	690	/
	18.2	26/30	821	

Estimation of sediment thicknesses are carried out using empirical equation (6) for all ground fundamental frequencies obtained, and the computed results are tabulated in Table 9. Besides, the percentage of different is also calculated by taking 16.7 m depth as the datum line for reliability of the prediction made.

$$h \text{ (in meter)} = 135.19 f_0^{-1.9791} \quad (6)$$

Finally, most of the passing frequencies have shown in good agreement when the maximum rates of underestimated percentages only indicated from 18.8% to 0.5%, compared to overestimated percentages from only 14% to 6.5%. Close approximation has increased the tendency of microtremor

analysis to become a reliable tool for rough estimation of sedimentary cover in the fastest way.

Table 9 Estimation of sediment thickness from the ground fundamental frequencies

File No.	Sensor No.	Natural Frequencies, f_0 (Hz)	Criteria: Passed, Failed or Recommended to be Repeated	Sediment thickness, h (m)	Diff. (%)
561-NS	S1	3.20	Passed	13.6	-18.8
	S2	2.69	Passed	19.0	14.0
	S3	3.42	Failed	11.8	-29.1
561-EW	S1	2.98	Failed	15.5	-7.0
	S2	2.88	Passed	16.6	-0.5
	S3	2.98	Passed	15.5	-7.0
597-NS	S1	2.88	Passed	16.6	-0.5
	S2	2.79	Failed	17.8	6.5
	S3	3.20	Failed	13.6	-18.8
597-EW	S1	2.79	Passed	17.8	6.5
	S2	2.79	Failed	17.8	6.5
	S3	2.88	Passed	16.6	-0.5

F. Estimation of Base Shear Force using ESA

A few assumptions have been applied including some extracted data from standard school constructions drawing obtained from Public Works Department of Malaysia (JKR). Besides, other considerations were also made according to standard design practice of British Standard since most of existing conventional structures in Malaysia were designed to this standard. Table 10 shows the design data applied in the calculations in terms of building configurations, material properties and other assumptions.

Table 10 Building design data

Dimensions and sizes	Total bay	20
	Storey height	3.60 m
	Bay spacing	3.00 m
	Building width	7.50 m
	Corridor slab width	2.10 m
	Parapet wall height	1.05 m
Slab	Thickness	150 mm
	Concrete density	24 kN/m ³
	Finishing	1.0 kN/m ²
Brickwall	Thickness	150 mm
	Plastering	20 mm/side
	Clay brick density	26 kN/m ³
	Mortar density	21 kN/m ³
Q_k	Imposed load	Refer Table 1.

Since none of a national seismic code yet introduced in this country, a seismic design code of Eurocode 8 [2] has been referred for estimation of the building base shear force. The following calculations are totally based on the expressions as provided from this code of practice and other related supplementary Eurocode standards.

The total mass (in tonne) from every building level was calculated based on equation (7), which taken from clause 3.2.4 Eurocode 8 [2]. Every floor from the ground level until roof have been calculated by taking the combination coefficient for variable action, $\Psi_{E,i}$, equal to 0.24 (where $\Psi_{E,i} = \phi \cdot \Psi_{2i}$ with $\phi = 0.8$ and $\Psi_{2i} = 0.3$). The summary of seismic masses calculated for each level is given in Table 11.

$$G_k + \Psi_{E,i} \cdot Q_k \text{ (in kN)} \quad (7)$$

Table 11 Seismic mass of SK Sri Molek building

Level	G _k (kN)	Q _k (kN)	G _k + Ψ _{E,i} Q _k (kN)	Mass (tonne)
Roof	230.4	576.0	368.6	37.6
3	5,020.4	1,626.8	5,410.8	551.6
2	4,820.6	1,986.8	5,297.4	540.0
1	4,820.6	1,998.0	5,300.1	540.3
GF	4,970.7	1,615.5	5,358.4	546.2
Total seismic mass, m				2,216.3

By taking 4.20 to 4.35 Hz (or 0.23 to 0.24 s of natural period, T_M) obtained from microtremor measurement, the site may be categorized in $T_B \leq T \leq T_C$. As described in clause 3.2.2.2 in Eurocode 8 [2], the elastic response spectrum $S_e(T_M)$, can be calculated by using equation (8) with all variables taken as given in Table 12. The calculated $S_e(T_M)$ shows 0.32 m/s² which similar to the peak acceleration value given by the design response spectrum curve as in Fig. 4, for T_M between 0.23 to 0.24 s.

$$S_e(T) = a_g \cdot S \cdot \eta \cdot 2.5 \quad (8)$$

Table 12 Computed values of $S_e(T)$

Variables	Value	Remarks
a_g : design ground acceleration	0.095 m/s ²	See Fig. 4
η : damping correction factor	1	Assume for viscous damping of 5%
S : soil factor	1.35	Assume type C with N_{SPT} value of 15 to 50 occurred approximately at 30 m depth

As stated in expression 4.5 from Eurocode 8 [2], the base shear force can be determined by equation (7), when λ is assumed 0.85 due to T_M is lesser than $2T_C$. From Fig. 4 again, T_C is identified close to 0.4 s.

$$F = S_e(T_M) \cdot m \cdot \lambda \quad (7)$$

In the end of this calculation, it shows that the estimated base shear force may achieve up to 602.8 kN which bigger than 1.5 % provision of notional horizontal load as stated in clause 3.1.4.2 from BS 8110 [3].

V. CONCLUSIONS

Integration of geophysical method, some empirical equations provided from previous studies and standard design code of practices may give bigger perspective in re-evaluation of dynamic characteristics and seismic vulnerability assessment of existing non-seismically design RC structure. This methodology can also benefit for a structure or site which lack of specific design database due to poor managing record system or the structure is too old. However, verification via reasonable methods should be carried out in order to produce a significant and reliable finding.

In this study, the dynamic characteristics and seismic vulnerability assessment of primary school RC building of SK Sri Molek has shown to successful prediction by using integration methods of microtremor technique, standard codes of practices and some previous empirical equations. The predominant frequencies of building are determined between 4.20 to 4.35 Hz in transverse and longitudinal directions, whereby the highest top displacement occurs on the upper floor and reducing when lowering to the ground level. The influence of bigger imposed load that mostly concentrated in the mid-span and farther from the staircases (may react as bracing member) has increased the translation displacement amplitude in transverse direction at C11, but these amplitudes are reducing when approaching to C1 and C21.

Meanwhile, the fundamental frequencies of site indicated between 2.69 to 3.20 Hz with maximum A_o of 7.78 in the NS direction and, 2.79 to 2.98 Hz at 7.46 of A_o in the EW direction. Reliability and clarity checking are also performed as recommended by SESAME [13] guideline. In terms of resonance potential of site-structure, it is expected to be classified in moderate level that could be occurred under equal oscillation between building and ground frequencies, under strong ground shaking and may lead to structural damages.

Valid verifications have been shown from the assessment of HVSR curve patterns, the ground fundamental frequencies and amplification factors values produced, with aid from some empirical equations of shear wave velocity and sediment thickness as well as the geotechnical data. Quick understanding on the overall picture of the subsurface soil profile, soil stiffness and sedimentary cover can also be roughly estimated from these ambient vibration findings.

From the estimation of total base shear force to Eurocode 8 [2] has indicated that, the notional design ultimate horizontal load for conventional load combination design applied in BS 8110 [3] against the existing structure has been exceeded, with the design response spectrum in Kuala Lumpur was adopted from the extreme earthquake experience ever recorded at 9.3 earthquake magnitude and 530 km of epicenter distance.

Even most expectations have been made that the survival of existing low-rise structure is higher if compared to the high-rise building under the earthquake threat, but the possibility of structural damages and casualties should not be underestimated since building durability, site-structure resonance effect, poor soil conditions etc. could become one of the main factor contributing to the structural disaster, especially for a building without seismic design provision.

ACKNOWLEDGMENT

The authors would like to acknowledge the financial support provided by Ministry of Education Malaysia (Higher Education) under ERGS grant 011. We are grateful to Universiti Tun Hussein Onn Malaysia for the equipment and facilities, JKR, District Education Office of Batu Pahat and SK Sri Molek administration for their priceless co-operation along the period of this research being conducted.

REFERENCES

- [1] Looi, T.W., Hee, M.C., Tsang, H.H. and Lam, N.T.K., "Recommended Earthquake loading model for Peninsular Malaysia," *Jurutera: Civil and Structural Engineering*, Vol 2013 No.4. ISSN 0126-9909, pp. 6-20, 2013.
- [2] *Design of Structures for Earthquake Resistance: General Rules, Seismic Actions and Rules for Buildings*, Brussels, European: EC 8: Part 1, Eurocode 8, 2003.
- [3] *Structural Use of Concrete, Code of Practice for Design and Construction*, London: BS 8110: Part 1, British Standards Institution, 1997.
- [4] Koong, N.K and Won, L.K., "Earthquake Hazard and Basic Concepts of Seismic Resistant Design of Structure. Master Builders," 4th Quarter, pp. 90-95, 2005.
- [5] Adnan, A., Marto, A., and Hendriyawan, "Lesson learned from the effect of recent far field Sumatra earthquakes to Peninsular Malaysia," presented at the 13th World Conference on Earthquake Engineering, B.C., Paper No. 416. Canada: Vancouver, 2004.
- [6] Megawati, K., Pan, T.C. & Koketsu, K., "Response spectral attenuation relationship for Sumatran-subduction earthquake and the seismic hazard implications to Singapore and Kuala Lumpur," *Soil Dynamics and Earthquake Engineering*, 25, pp.11-25, 2005.
- [7] Pan, T.C., "Estimation of peak ground acceleration of the Malay Peninsula due to distant Sumatran," *GeoForschungs Zentrum Potsdam*. Germany: Scientific Technical Report STR98/14, pp. 340 – 359, 1998.
- [8] Mukherjee, A. and Joshi, M., "FRPC reinforced concrete beam-column joints under cyclic excitation," *Composite Structures*, 70, pp. 185-199, 2005.
- [9] Balendra, T. and Li, Z., "Seismic Hazard of Singapore and Malaysia," *EJSE Special Issue: Earthquake Engineering in the low and moderate seismic regions of Southeast Asia and Australia*, pp. 57-63, 2008.
- [10] Flores, J., Novaro, O., and Seligman, T.H., "Possible resonance effect in the distribution of earthquake damage in Mexico City," *Nature*, 326, pp. 783-785, 1987.
- [11] Ivanovic, S.S., Trifunac, M.D., Novikova, E.I., Gladkov, A.A. and Todorovska, M.I., "Ambient vibration tests of a seven-story reinforced concrete building in Van Nuys, California, damaged by the 1994 Northridge earthquake," *Soil Dynamics and Earthquake Engineering*, 19, pp. 391 – 411, 2000.
- [12] Gioncu, V. and Mazzolani, F., *Earthquake engineering for structural design*, New York: Spon Press, pp. 1-527, 2011.
- [13] SESAME, "Guidelines for the implementation of the H/V spectral ratio technique on ambient vibrations: measurements, processing and interpretation," European Commission – Research General Directorate Project No. EVG1-CT-2000-00026, 2004.
- [14] Gosar, A., "Microtremor soil-structure resonance in the Bovec Basin (NW Slovenia) related to 1998 and 2004 damaging earthquake," in Mucciarelli, M., Herak, M. and Cassidy, J., *Increasing Seismic Safety by Combining Engineering Technologies and Seismological Data*, Netherlands: Springer, pp. 241-279, 2009.
- [15] Nakamura, Y., "Clear identification of fundamental idea of Nakamura's techniques and its applications," presented at the Twelfth World Conference on Earthquake Engineering, New Zealand, pp. 1-8, 2000.
- [16] Sato, T, Nakamura, Y. and Saita, J., "Evaluation of the amplification characteristics of subsurface using microtremor and strong motion – the studies at Mexico City," presented at the 13th World Conference on Earthquake Engineering, Paper No. 862, Canada: Vancouver, 2004.
- [17] Dwa Desa Warnana, Triwulan, Sungkono, Widya Utama, "Assessment to the soil-structure resonance using microtremor analysis on Pare - East Java, Indonesia," *Asian Transactions on Engineering (ATE ISSN: 2221-4267)* Volume 01, Issue 04, pp. 6-12, 2011.
- [18] *Loading for buildings-Code of practice for dead and imposed loads*. London: BS 6399: Part 1, British Standards Institution, 1996.
- [19] Marek, A.R., Bray, J.D., Abrahamson, N.A., "An empirical geotechnical seismic site response procedure," in Mucciarelli, M., Herak, M. and Cassidy, J., *Increasing Seismic Safety by Combining Engineering Technologies and Seismological Data*, Netherlands: Springer, pp. 353-380, 2009.
- [20] Gosar, A., "Site effects and soil-structure resonance study in the Kobarid basin (NW Slovenia) using microtremors," *Nat. Hazards Earth Syst. Sci.* 10, pp. 761-772, 2010.
- [21] Masi, A and Vona, M., "Estimation of the period vibration of existing RC building types Based on experimental data and numerical result," in Mucciarelli, M., Herak, M. and Cassidy, J., *Increasing Seismic Safety by Combining Engineering Technologies and Seismological Data*, Netherlands: Springer, pp. 207-225, 2009.
- [22] Gosar, A., "Microtremor study of site effects and soil-structure resonance in The City Of Ljubljana (central Slovenia)," *Bull. Earthquake Eng.* 8, pp. 571-592, 2010.
- [23] IKRAM Group Sdn. Bhd., "Laporan Akhir Penyiasatan Tapak untuk Cadangan Membina Bangunan Gantian di Sekolah Kebangsaan Sri Molek, Batu Pahat Johor. Malaysia," SI Report, 2008.
- [24] Jun, Y., "Frequency-dependent amplification of unsaturated surface soil layer," *Journal Geotech and Geoenvironmental Engineering*, 132, pp. 526-531, 2006.
- [25] Motamed, R., Ghalandarzadeh, A., Tawhata, I. and Tabatabaei, S.H., "Seismic microzonation and damage assessment of Bam City, Southern Iran," *Journal of Earthquake Engineering*, 11, pp. 110-132, 2007.
- [26] Dinesh, B.V., Nair, G.J., Prasad, A.G.V., Nakkeeran, P.V. and Radhakrishna, M.C., "Estimation of sedimentary layer shear wave velocity using micro-tremor H/V ratio measurements for Bangalore city," *Soil Dynamics and Earthquake Engineering* 30, pp. 1377-1382, 2010.